JOURNAL OF GEOPHYSICAL RESEARCH, VOL. 103, NO. A9, PAGES 20,487–20,500, SEPTEMBER 1, 1998

Relativistic theory of wave-particle resonant diffusion with application to electron acceleration in the magnetosphere

Danny Summers

Department of Mathematics and Statistics, Memorial University of Newfoundland, St. John's Canada

Richard M. Thorne

Department of Atmospheric Sciences, University of California, Los Angeles

Fuliang Xiao

Department of Physics and Astronomy, University of California, Los Angeles

Abstract. Resonant diffusion curves for electron cyclotron resonance with field-aligned electromagnetic R mode and L mode electromagnetic ion cyclotron (EMIC) waves are constructed using a fully relativistic treatment. Analytical solutions are derived for the case of a single-ion plasma, and a numerical scheme is developed for the more realistic case of a multi-ion plasma. Diffusion curves are presented for plasma parameters representative of the Earth's magnetosphere at locations both inside and outside the plasmapause. The results obtained indicate minimal electron energy change along the diffusion curves for resonant interaction with L mode waves. Intense storm time EMIC waves are therefore ineffective for electron stochastic acceleration, although these waves could induce rapid pitch angle scattering for $\gtrsim$ 1 MeV electrons near the duskside plasmapause. In contrast, significant energy change can occur along the diffusion curves for interaction between resonant electrons and whistler (R mode) waves. The energy change is most pronounced in regions of low plasma density. This suggests that whistler mode waves could provide a viable mechanism for electron acceleration from energies near 100 keV to above 1 MeV in the region outside the plasmapause during the recovery phase of geomagnetic storms. A model is proposed to account for the observed variations in the flux and pitch angle distribution of relativistic electrons during geomagnetic storms by combining pitch angle scattering by intense EMIC waves and energy diffusion during cyclotron resonant interaction with whistler mode chorus outside the plasmasphere.

1. Introduction

The flux of outer radiation zone relativistic ($\gtrsim$ 1 MeV) electrons exhibits considerable variability during geomagnetic storms [e.g., *Baker et al.*, 1986; 1994]. Characteristically, there is a sharp depletion during the onset of the storm, and this is often followed by a gradual increase (over days) to flux levels well above prestorm values during the recovery phase [*Baker et al.*, 1986; *Li et al.*, 1997a]. The increase in relativistic electron flux during a storm is strongly correlated with fast solar wind streams and prolonged periods of southward directed interplanetary magnetic field [*Paulikas and Blake*, 1979; *Blake et al.*, 1997]. This suggests that enhanced magnetospheric convection is a necessary condition for subsequent electron acceleration to relativistic (> 1 MeV) energies.

While enhanced convective activity can lead to a pronounced increase in the flux of 10–100-keV electrons during storms, it is unlikely that this process can yield electron energies in excess of the typical potential drop across the magnetosphere ($\approx$ a few 100 keV). Enhanced fluxes of $\gtrsim$ 1 MeV electrons during the storm recov-

Paper number 98JA01740.
0148-0227/98/98JA-01740$09.00

ery must therefore be attributed to additional acceleration processes. Betatron acceleration, associated with inward radial diffusion [*Schulz and Lanzerotti*, 1974], could contribute to electron energization during storms [e.g., *Li et al.*, 1997a]. However, the acceleration to highly relativistic energies ($\geq$ 300 MeV/G) appears to be located deep within the magnetosphere, since the phase space density of such electrons has a peak near $L = 5$ during storms (R. S. Selesnick and J. B. Blake, Observational constraints on the location of radiation belt electron acceleration, submitted to *Journal of Geophysical Research*, 1998). Furthermore, the phase space density in the solar wind is insufficient to account for the observed outer zone fluxes during a storm [*Li et al.*, 1997b]. This would appear to rule out the simple concept of inward radial diffusion from a source region in the geomagnetic tail or near the magnetopause boundary as a viable mechanism to account for the gradual increase in relativistic flux during the storm recovery.

Multi dimension diffusion, which leads to a recycling of energetic electrons [e.g., *Nishida* 1976], could still be important, but this process has yet to be quantified. The present investigation will therefore explore the potential for local stochastic acceleration by plasma waves. The basic concept of energy diffusion of relativistic electrons resulting from resonant interaction with whistler mode waves in the magnetosphere has previously been discussed by *Temerin et al.* [1994] and *Li et al.* [1997a]. Such processes will be quantified here and the analysis will be applied to both right and left polarized waves. The gradual acceleration process (occurring over days) addressed in this paper is distinct from the rapid increase in energetic electron flux associated with inductive electric fields, which has been previously discussed, for example, by *Li et al.* [1993].

Horne and Thorne [1998] have identified potential wave modes that are capable of resonating with electrons over the important energy range from 100 keV to a few MeV in different regions of the Earth's magnetosphere. The principal waves are L mode electromagnetic ion cyclotron (EMIC) waves, oblique magnetosonic waves and R mode whistlers. In this paper the resonant diffusion curves, along which the electrons are forced to move during cyclotron resonant interaction with both R and L mode electromagnetic waves, will be determined for fully relativistic energies. The energy change along the diffusion curves provides a measure of the potential for stochastic electron acceleration by each wave mode. The results are parameterized in terms of the wave frequency, wave polarization (R mode or L mode) and local Alfvén speed. A brief account of the concept of a resonant diffusion curve for a relativistic plasma is given in section 2. The general resonant condition for relativistic electron interaction with field-aligned R mode and L mode electromagnetic waves is given in section 3. Simple dispersion relations for such waves in a cold plasma are presented in section 4. A detailed analysis of the curves in velocity space along which relativistic electrons are constrained to move during resonant interaction with each wave mode is provided in section 5. An exact analytical solution is obtained for the case of a single-ion cold plasma, and a numerical scheme is used to determine the diffusion curves for the more general case of a multi-ion plasma. For completeness, solutions obtained under the nonrelativistic approximation are given in section 6. Numerical solutions for the electron diffusion curves, for each wave mode and under a variety of different magnetospheric conditions are presented in section 7. In section 8 a model is presented to account for the acceleration of relativistic electrons during storms, based on numerical solutions for the diffusion curves and available information on storm time wave characteristics. The main conclusions of this study are summarized in section 9.

2. Resonant Diffusion Curves

Gendrin [1968, 1981] and *Gendrin and Roux* [1980] have provided a detailed analysis of resonant charged-particle diffusion and its relationship with wave growth and damping, although the theory was developed only for a nonrelativistic plasma. More recently, *Walker* [1993] has considered resonant diffusion including relativistic effects, but his analysis was restricted to the case of a single-wave characteristic associated with a wave of a particular frequency. In this section we develop the differential equation for the curves in $(v_{||}, v_{\perp})$ space along which the resonant particles diffuse under the influence of a broad spectrum of electromagnetic waves. The parallel and perpendicular suffixes denote directions parallel and perpendicular to a given ambient magnetic field. Following *Walker* [1993], we note that in a frame $(v_{||}', v_{\perp}')$ moving with the phase velocity of the wave (the "wave frame"), the relativistic kinetic energy of the resonant particle is conserved, that is,

$$v_{||}' dv_{||}' + v_{\perp}' dv_{\perp}' = 0. \tag{1}$$

For frames moving with a relative velocity u_{ph}, the wave phase velocity along the magnetic field, the Lorenz transformation is

$$\begin{aligned} v_{||}' &= \frac{v_{||} - u_{ph}}{[1 - v_{||} u_{ph}/c^2]}, \\ v_{\perp}' &= \frac{[1 - u_{ph}^2/c^2]^{1/2} v_{\perp}}{[1 - v_{||} u_{ph}/c^2]}, \end{aligned} \tag{2}$$

where c is the speed of light. Substitution of (2) into (1) leads, after some manipulation, to the result,

$$[1 - \frac{v_{||} u_{ph}}{c^2}] v_{\perp} dv_{\perp} + [v_{||} - u_{ph} + \frac{u_{ph} v_{\perp}^2}{c^2}] dv_{||} = 0. \tag{3}$$

Equation (3) is the differential equation for the resonant diffusion curves in the $(v_{||}, v_{\perp})$ plane, taking

full account of relativistic effects. By formally setting $c \rightarrow \infty$, the well-known nonrelativistic result is recovered, namely,

$$v_\perp dv_\perp + [v_{||} - u_{ph}]dv_{||} = 0. \quad (4)$$

In the derivation of (3), it has been implicitly assumed that $u_{ph}/c < 1$, and this restriction will be retained for the remainder of this paper. However, it should be noted that the result for a single-wave characteristic was shown by *Walker* [1993] to be valid for arbitrary values of the phase velocity u_{ph}. It is convenient to measure all velocities in units of c, so we write $v_{||}/c \rightarrow v_{||}, v_\perp/c \rightarrow v_\perp$, and $u_{ph}/c \rightarrow u$; equation (3) then assumes the dimensionless form,

$$(1 - uv_{||})v_\perp dv_\perp + (v_{||} - u + uv_\perp^2)dv_{||} = 0. \quad (5)$$

In general, u is a function of wave frequency and so integration of (5) is nontrivial. In the special case that $u = \text{const} = u_0$, (5) can be integrated to recover the form of the single-wave characteristic given by *Walker* [1993], namely,

$$(1-u_0^2v_0^2)v_{||}^2 - 2u_0(1-v_0^2)v_{||} + (1-u_0^2)v_\perp^2 = v_0^2 - u_0^2, \quad (6)$$

where v_0 is a constant of integration. For given values of u_0 and v_0 (with $u_0 < 1$ and $v_0 < 1$), (6) in general represents an ellipse with center $(v_{||} = u_0(1 - v_0^2)/(1 - u_0^2v_0^2), v_\perp = 0)$; the major axis is parallel to the $v_\perp$ axis and the minor axis is coincident with the $v_{||}$ axis. More precisely, the required diffusion curve is the semiellipse portion of (6) in the upper half-plane ($v_\perp \geq 0$). Thus (5) may be interpreted geometrically as requiring a resonant particle to move in the $(v_{||}, v_\perp)$ plane along a diffusion curve, every point of which is tangential to some single-wave characteristic ellipse of the form (6).

3. Resonance Conditions

In the kinetic theory of wave-particle interaction in a relativistic plasma, the general resonance condition is

$$\omega - kv_{||} = n\Omega_\sigma(1 - v^2/c^2)^{1/2}, \quad (7)$$

where $v = (v_{||}^2 + v_\perp^2)^{1/2}$ is the particle velocity, ω is the wave frequency, k is the wave number in the direction of propagation, n $(= 0, \pm 1, \pm 2, ...)$ is an integer denoting the cyclotron harmonic, and $\Omega_\sigma = q_\sigma B_0/(m_\sigma c)$ is the particle gyrofrequency with q_σ the particle charge (including sign), m_σ is the particle rest mass, and B_0 is the magnetic field strength. For electron interaction with electromagnetic R mode and L mode waves propagating parallel to the magnetic field, only the first-order $(n = \pm 1)$ cyclotron resonance can occur, and (7) becomes

$$\omega - kv_{||} = \pm|\Omega_e|(1 - v^2/c^2)^{1/2}, \quad (8)$$

where the plus and minus signs refer to the R and L modes, respectively, and $|\Omega_e| = eB_0/(m_e c)$, where e is the electron charge and m_e the electron rest mass. For resonance with R mode waves, it is convenient to normalize the wave frequency in units of $|\Omega_e|$, so we set $\omega/|\Omega_e| \rightarrow \omega$ and write (8) as

$$v_{||} = -u[\frac{1}{\omega}(1 - v_{||}^2 - v_\perp^2)^{1/2} - 1]. \quad (9)$$

For resonance with L mode waves, we similarly set $\omega/\Omega_i \rightarrow \omega$, where $\Omega_i = eB_0/(m_p c)$, with m_p the proton rest mass; (8) may then be written as

$$v_{||} = u[\frac{1}{\epsilon\omega}(1 - v_{||}^2 - v_\perp^2)^{1/2} + 1] \quad (10)$$

where $\epsilon = m_e/m_p$.

For fixed values of ω and u the dimensionless forms of the resonance conditions (9) or (10) are represented by semiellipses in the upper half-plane ($v_\perp \geq 0$). For the R mode resonance the center is $(v_{||} = u\omega^2/(u^2+\omega^2), v_\perp = 0)$; and for the L mode the center is $(v_{||} = u\epsilon^2\omega^2/(u^2 + \epsilon^2\omega^2), v_\perp = 0)$. In both cases, the major axis is parallel to the $v_\perp$ axis and the minor axis is coincident with the $v_{||}$ axis. Also, in both cases, the semiellipses meet the light semi-circle $(v^2 = 1, v_\perp \geq 0)$ tangentially at the point $(v_{||} = u, v_\perp = (1 - u^2)^{1/2})$.

4. Wave Dispersion Relations

The standard cold plasma dispersion relations in an electron-proton plasma for parallel-propagating electromagnetic waves are given by [e.g., *Stix*, 1962; *Swanson*, 1989],

$$\frac{c^2k^2}{\omega^2} = 1 - \frac{\omega_{pe}^2}{\omega(\omega \mp |\Omega_e|)} - \frac{\omega_{pi}^2}{\omega(\omega \pm \Omega_i)} \quad (11)$$

where the upper sign combination refers to the R mode and the lower one to the L mode, $\omega_{pe} = (4\pi N_0 e^2/m_e)^{1/2}$ is the electron plasma frequency, $\omega_{pi} = (4\pi N_0 e^2/m_p)^{1/2}$ is the proton plasma frequency, and N_0 is the electron/proton number density. By using the aforementioned dimensionless variables, the R mode dispersion relation can be written

$$u^2 = \frac{\alpha(1 - \omega)(\omega + \epsilon)}{\alpha(1 - \omega)(\omega + \epsilon) + 1 + \epsilon} \quad (12)$$

and the L mode dispersion relation is

$$u^2 = \frac{\alpha\epsilon(1 + \epsilon\omega)(1 - \omega)}{\alpha\epsilon(1 + \epsilon\omega)(1 - \omega) + 1 + \epsilon}, \quad (13)$$

where the nondimensional parameter

$$\alpha = \frac{\Omega_e^2}{\omega_{pe}^2} = \frac{m_p}{m_e}\frac{V_A^2}{c^2} \quad (14)$$

has been introduced; V_A is the Alfvén speed given by $V_A^2 = B_0^2/(4\pi N_0 m_p)$. Throughout the remainder of this

paper ω is used to denote $\omega/|\Omega_e|$ for the R mode and ω/Ω_i for the L mode.

Useful approximate forms of (12) and (13) are

$$u^2 = \alpha\omega(1-\omega) \tag{15}$$

$$u^2 = \alpha\epsilon(1-\omega). \tag{16}$$

respectively. Equation (15) is the standard whistler mode dispersion relation, valid for R mode waves in the frequency range $\epsilon << \omega < 1$, obtained by omitting the first term (the one) and the last term (due to ions) on the right-hand side of (11). Equation (16) is the Alfvén wave dispersion relation, which is approximately valid for L mode waves with frequencies below the proton gyrofrequency Ω_i in a single-ion plasma.

The case of electromagnetic L mode waves in a multi-ion plasma, specifically a plasma containing both helium and oxygen ions in addition to hydrogen ions, is of more general interest. The relevant dispersion relation is

$$\frac{c^2k^2}{\omega^2} = 1 - \frac{\omega_{pe}^2}{\omega(\omega+|\Omega_e|)} - \sum_{\ell=1}^{3}\frac{\omega_{p\ell}^2}{\omega(\omega-\Omega_\ell)}, \tag{17}$$

where the suffix ℓ denotes the ion species; the values $\ell = 1,2,3$ refer to hydrogen (H^+), helium (He^+), and oxygen (O^+), respectively. Here $\omega_{pl} = (4\pi N_\ell q_\ell^2/m_\ell)^{1/2}$ is the ion plasma frequency and $\Omega_\ell = q_\ell B_0/(m_\ell c)$ is the ion gyrofrequency, with $q_1 = q_2 = q_3 = e$, $m_1 = m_p, m_2 = 4m_p$, and $m_3 = 16m_p$. Charge neutrality requires that $N_1 + N_2 + N_3 = N_0$, where N_0 is the electron number density. Equation (17) can be expressed in the dimensionless form

$$\frac{1}{u^2} = 1 - \frac{1}{\alpha\epsilon\omega}\left(\frac{1}{1+\epsilon\omega} + \frac{\eta_1}{\omega-1} + \frac{\eta_2}{4\omega-1} + \frac{\eta_3}{16\omega-1}\right) \tag{18}$$

where the fractional composition of the ion species in the plasma, $\eta_1 = N_1/N_0$, $\eta_2 = N_2/N_0$, and $\eta_3 = N_3/N_0$, is such that $\eta_1 + \eta_2 + \eta_3 = 1$. It is convenient to rewrite (18) in the form

$$u^2 = \frac{\alpha\epsilon P}{\alpha\epsilon P + p_1\omega^2 + p_2\omega + p_3}, \tag{19}$$

where

$$P = (1+\epsilon\omega)(1-\omega)(4\omega-1)(16\omega-1) \tag{20}$$

$$\begin{aligned} p_1 &= 64 + \epsilon(64\eta_1 + 16\eta_2 + 4\eta_3), \\ p_2 &= -84 + (64-20\epsilon)\eta_1 + (16-17\epsilon)\eta_2 + (4-5\epsilon)\eta_3, \\ p_3 &= 21 + \epsilon - (20\eta_1 + 17\eta_2 + 5\eta_3). \end{aligned} \tag{21}$$

In the special case that $\eta_1 = 1$ and $\eta_2 = \eta_3 = 0$, the dispersion relation (19) reduces to the single-ion relation (13).

5. Analysis

A principal objective of this study is to determine the curves in the plasma frame $(v_{||}, v_\perp)$ along which the electrons diffuse under the influence of resonant scattering by electromagnetic R mode and L mode waves. This requires a solution of the diffusion equation (5) together with a resonance condition (equation (9) or (10)), subject to a specified dispersion relation $u(\omega)$. A solution $v_{||} = v_{||}(\omega), v_\perp = v_\perp(\omega)$ of such a system will be sought in parametric form with the (dimensionless) frequency ω as the parameter. By rewriting the diffusion equation (5) as

$$(1-uv_{||})\frac{d}{d\omega}(v_\perp^2) = -2(v_{||} - u + uv_\perp^2)\frac{dv_{||}}{d\omega}, \tag{22}$$

where $u = u(\omega)$, the resonance condition (9) (or (10)) can be solved for $v_\perp^2$ and used in (22) to obtain the following equation that involves $v_{||}$ only:

$$\frac{dv_{||}}{d\omega} = \left(\frac{1-uv_{||}}{1-u^2}\right)\left[\frac{v_{||}}{u}\frac{du}{d\omega} - \frac{(v_{||}-u)}{\omega}\right]. \tag{23}$$

Since u is a specified function of ω, given by a dispersion equation from section 4, (23) determines $v_{||} = v_{||}(\omega)$ completely, subject to appropriate boundary/initial conditions. Equation (23) is itself valid for both R and L mode resonance scattering. The corresponding solution for $v_\perp = v_\perp(\omega)$ is given by

$$v_\perp = [1 - v_{||}^2 - \frac{\omega^2}{u^2}(v_{||}-u)^2]^{1/2} \tag{24}$$

for R mode waves, using (9), and by

$$v_\perp = [1 - v_{||}^2 - \frac{\epsilon^2\omega^2}{u^2}(v_{||}-u)^2]^{1/2} \tag{25}$$

for L mode waves, using (10).

It is useful to express (23) in the form

$$\frac{dv_{||}}{d\omega} = p(\omega)v_{||}^2 + q(\omega)v_{||} + r(\omega) \tag{26}$$

where

$$\begin{aligned} p(\omega) &= \frac{1}{(1-u^2)}\left(\frac{u}{\omega} - \frac{du}{d\omega}\right), \\ q(\omega) &= \frac{1}{(1-u^2)}\left(\frac{1}{u}\frac{du}{d\omega} - \frac{u^2}{\omega} - \frac{1}{\omega}\right), \\ r(\omega) &= \frac{u}{\omega(1-u^2)}. \end{aligned} \tag{27}$$

Equation (26) can be recognized as a well-known nonlinear differential equation, the Riccati equation, which may be solved "completely" if a particular solution is known. By inspection, it can be seen that $v_{||} = u$ is a

particular solution of (26). Proceeding with the standard method of solution [e.g., *Ince*, 1944], we substitute

$$v_{||} = u + \frac{1}{V} \tag{28}$$

into (26) to obtain a linear equation for the function $V(\omega)$, namely,

$$\frac{d}{d\omega}\,(g(\omega)V) = -g(\omega)p(\omega), \tag{29}$$

where

$$g(\omega) = e^{\int (2pu+q)d\omega}. \tag{30}$$

By using the expressions for p and q from (27), the function g can be evaluated explicitly as

$$g(\omega) = u(1-u^2)^{1/2}/\omega. \tag{31}$$

Equation (29) can be easily solved for $V = (v_{||} - u)^{-1}$ in the form

$$g(\omega)V = K - f(\omega), \tag{32}$$

where K is a constant of integration and

$$f(\omega) = \int g(\omega)p(\omega)d\omega = \int \frac{u^2\{1 - \frac{\omega}{u}\frac{du}{d\omega}\}d\omega}{\omega^2(1-u^2)^{1/2}}\,. \tag{33}$$

Finally, from (32) the solution for $v_{||}$ can be written

$$v_{||} = u + \frac{g(\omega)}{K - f(\omega)}\,. \tag{34}$$

Solution (34) is valid for an arbitrarily specified phase-speed function $u(\omega)$; g is given by (31) and f by the integral (33). As noted above, the corresponding solution for $v_\perp$ is then obtained from (24) for the R mode, and from (25) for the L mode. We determine the constant K by applying the boundary condition $v_{||} = v_{||c}, v_\perp = 0$ at the frequency $\omega = \omega_c$, where ω_c is a chosen value in the range $0 < \omega_c < 1$. Hence, from (34), we obtain

$$K = f(\omega_c) + \frac{g(\omega_c)}{v_{||c} - u_c}\,, \tag{35}$$

where $u_c = u(\omega_c)$. From the R mode resonance condition (24), it follows that

$$v_{||c} = \frac{u_c\{\omega_c^2 - [u_c^4 + (\omega_c^2 + u_c^2)(1-u_c^2)]^{1/2}\}}{(\omega_c^2 + u_c^2)} \tag{36}$$

(and it can be shown here that $v_{||c} < 0$ always), while from the L mode resonance condition (25) it follows that

$$v_{||c} = \frac{u_c\{\epsilon^2\omega_c^2 + [u_c^4 + (\epsilon^2\omega_c^2 + u_c^2)(1-u_c^2)]^{1/2}\}}{(\epsilon^2\omega_c^2 + u_c^2)} \tag{37}$$

(and clearly $v_{||c} > 0$ in this case).

The problem of finding the resonant diffusion curve for an arbitrary function $u(\omega)$ has thus been reduced to one involving a single quadrature. In cases where the integral (33) can be evaluated in closed form, the diffusion curve can be calculated explicitly in analytical form. When the integral (33) is difficult or impossible to evaluate in closed form, this integral can always be evaluated by a technique of numerical quadrature. Alternatively, the differential equation (23) for $v_{||}$ can in all cases be directly integrated numerically, subject, say, to the initial condition $v_{||} = v_{||c}$ at $\omega = \omega_c$.

Corresponding to both the simplified R mode dispersion relation (15) and the simplified L mode dispersion relation (16), the integral (33) and hence the function $f(\omega)$ is readily evaluated; the functions f and g for the R mode (equation (15)) are given by

$$f(\omega) = -\frac{\alpha}{2}\,\log_e\left(\{2 - \alpha\omega + 2[1-\alpha\omega(1-\omega)]^{1/2}\}/(2\omega)\right), \tag{38}$$

$$g(\omega) = \{\alpha(1-\omega)[1-\alpha\omega(1-\omega)]/\omega\}^{1/2}, \tag{39}$$

while for the L mode (equation (16)) they are

$$f(\omega) = (\alpha\epsilon)^{1/2}\big([(1+a^2)/(2a^3)]\log_e\{[(\omega+a^2)^{1/2}+a]^2/\omega\} - (\omega+a^2)^{1/2}/(a^2\omega)\big), \tag{40}$$

$$g(\omega) = \{\alpha\epsilon(1-\omega)[1-\alpha\epsilon(1-\omega)]\}^{1/2}/\omega, \tag{41}$$

where $a = 1/(\alpha\epsilon) - 1$. The R mode solution corresponding to (38)–(39) is valid for $\alpha < 4$, while the L mode solution corresponding to (40)–(41) is valid for $\alpha\epsilon < 1$. These restrictions relate directly to the condition $u < 1$.

Evaluation of $f(\omega)$ for both the "full" (single-ion) R mode and L mode dispersion relations (12) and (13) is also straightforward, though tedious. Explicit forms for the functions f and g corresponding to each of the "full" dispersion equations (12) and (13) are presented in Appendix A. For the more general multi-ion dispersion relation (19), evaluation of the integral (33) is imprudent. In this case, we solve the differential equation (23) numerically for $v_{||}(\omega)$; the explicit form of (23) corresponding to the dispersion relation (19) is given in Appendix B.

6. Nonrelativistic Theory

For completeness, and also for comparison with the foregoing relativistic theory, we include a brief account of the determination of nonrelativistic resonant diffusion curves. In dimensionless form, the nonrelativistic diffusion equation (4) is

$$v_\perp dv_\perp + (v_{||} - u)dv_{||} = 0\,. \tag{42}$$

If the wave phase velocity is a constant, $u = u_0$, (42) has the integral

$$v_\perp^2 + (v_{||} - u_0)^2 = const. \tag{43}$$

Thus the single-wave characteristics are circles, centered at $(v_{||} = u_0, v_\perp = 0)$ [e.g., see *Kennel and Engelmann*, 1966; *Gendrin*, 1968]. However, in general, the phase velocity u is dependent on frequency, and so (42) must be integrated in conjunction with an attendant dispersion equation and a resonance condition. The R mode and L mode resonance conditions, corresponding to the non-relativistic versions of (9) and (10), are,

$$v_{||} = -u(\frac{1}{\omega} - 1) \tag{44}$$

$$v_{||} = u(\frac{1}{\epsilon\omega} + 1). \tag{45}$$

respectively. Accordingly, (42) must be solved simultaneously with either condition (44) or (45) and an appropriate dispersion relation (such as given in section 4). The nonrelativistic case is much simpler to analyze than the relativistic case. Following *Gendrin* [1968], we express (42) in the form

$$v_\perp dv_\perp + (v_{||} - u)d(v_{||} - u) + (v_{||} - u)du = 0. \tag{46}$$

Eliminating $(v_{||} - u)$ in the last term of (46) by use of (44) or (45) yields

$$v_\perp dv_\perp + (v_{||} - u)d(v_{||} - u) - \frac{u}{\omega}\, du = 0 \tag{47}$$

for the R mode interaction and

$$v_\perp dv_\perp + (v_{||} - u)d(v_{||} - u) + \frac{u}{\epsilon\omega}\, du = 0 \tag{48}$$

for the L mode interaction. Finally, (47) and (48) can be integrated to obtain the results

$$v_\perp = \left(\text{constant} + 2\int \frac{u}{\omega}\, du - \frac{u^2}{\omega^2}\right)^{1/2}, \tag{49}$$

$$v_\perp = \left(\text{constant} - \frac{2}{\epsilon}\int \frac{u}{\omega}\, du - \frac{u^2}{\epsilon^2\omega^2}\right)^{1/2}. \tag{50}$$

respectively. Thus, for any specified function $u(\omega)$, the desired solution for $v_{||}$ and $v_\perp$ in parametric form is given by (44) and (49) for the R mode, and by (45) and (50) for the L mode. By applying the boundary condition $v_\perp(\omega_c) = 0$, where ω_c is a chosen frequency, both R mode and L mode solutions can be written in the form

$$v_\perp = [F(\omega_c) - F(\omega)]^{1/2}, \tag{51}$$

$$v_{||} = G(\omega), \tag{52}$$

where the functions F and G are defined from (44), (45), (49), and (50). Corresponding to the simplified R mode dispersion relation (15), we find that

$$F(\omega) = \alpha[(1-\omega)/\omega + 2\omega - \log_e \omega], \tag{53}$$

$$G(\omega) = -(\alpha/\omega)^{1/2}(1-\omega)^{3/2}, \tag{54}$$

while for the simplified L mode dispersion relation (16), we find

$$F(\omega) = \alpha[(1-\omega)/(\epsilon\omega^2) - \log_e \omega], \tag{55}$$

$$G(w) = (\alpha/\epsilon)^{1/2}(1-\omega)^{1/2}(1+\epsilon\omega)/\omega. \tag{56}$$

The forms of the functions F and G corresponding to the "full" single-ion dispersion relations (12) and (13) are given in Appendix C. For cases in which the function u is such that the integral in (49) or (50) is very tedious to evaluate analytically, this integral can also be evaluated by numerical quadrature. Alternatively, the substitution of (44) or (45) in (42) yields equations for $v_\perp$ for the R mode and L mode,

$$\frac{d}{d\omega}(v_\perp^2) = \frac{2u^2}{\omega^3} - \frac{(1-\omega)}{\omega^2}\frac{d(u^2)}{d\omega}, \tag{57}$$

$$\frac{d}{d\omega}(v_\perp^2) = \frac{2u^2}{\epsilon^2\omega^3} - \frac{(1+\epsilon\omega)}{\epsilon^2\omega^2}\frac{d(u^2)}{d\omega}. \tag{58}$$

respectively. Equations (57) and (58) can be readily integrated numerically, subject to appropriate boundary conditions and chosen dispersion relations.

It is pertinent to note here that in a recent paper by *Thorne and Horne* [1996] an error was made in the calculation of the resonant diffusion curves in the nonrelativistic case (see their section 3). By an oversight, the equation of diffusion in the integral form (our (43)) was used by *Thorne and Horne* [1996] rather than the appropriate differential form (our equation (42)). Thus the analytical solution (5) given by *Thorne and Horne* [1996], as well as the diffusion curves shown in their Figure 2, are incorrect. Since the case considered by *Thorne and Horne* [1996] involves the whistler dispersion equation (their (3) and our (15)), the correct solution is given by our (51)–(54). Correct solution curves for the nonrelativistic case are presented below.

7. Numerical Solutions

The resonant diffusion curves in a relativistic plasma (as well as in a nonrelativistic plasma) are uniquely characterized by the parameter $\alpha = \Omega_e^2/\omega_{pe}^2$ and the ion composition. Representative values of α have been adopted to illustrate the range of diffusion curves possible for the case of resonant scattering by R mode and L mode waves. Typically, near the equatorial plane inside the Earth's high-density plasmasphere, $10^{-2} \leq \alpha \leq 10^{-1}$, while outside the plasmapause $\alpha \geq 0.25$. In the low-density auroral cavity at high altitudes, $\alpha > 10$. The results presented here are therefore restricted to the range $10^{-2} \leq \alpha \leq 10$.

7.1. R Mode Waves

Examples of the resonance ellipse (9) for the dominant first-order ($n = -1$) cyclotron resonance between relativistic electrons and R mode waves, described by the cold plasma dispersion relation (12), are shown in Figure 1. In each panel the resonance condition is shown for five distinct frequencies, $0.1 \leq \omega/|\Omega_e| \leq 0.9$. The parameter α, which determines the wave phase speed, leads to a significant change in resonant energy in the progression from a higher-density region (Figure 1a) to a lower density region (Figure 1c). All curves meet the light curve ($v^2 = 1$) when $v_{||} = u(\omega)$. In contrast to the nonrelativistic approximation (44), where $v_{||} < 0$, relativistic mass corrections to the resonance condition allow cyclotron resonant scattering over a sizable domain in velocity space with $v_{||} > 0$, especially for the case with $\alpha > 1$.

The corresponding diffusion curves, along which electrons are constrained to move during resonant scattering by R mode waves, are illustrated in Figure 2 for the case of a relatively high plasma density with $\alpha < 1$. These curves are constructed using the exact analytical solution given in Appendix A for the case of R mode waves in a cold single-ion plasma using the dispersion relation (12). The panels on the left show the diffusion curves in velocity space, while those on the right show the change in kinetic energy, $E_k = (\gamma - 1)m_e c^2$, measured in MeV, as a function of the normalized resonant wave frequency $\omega/|\Omega_e|$ along each curve. This pair of plots is constructed for three distinct values of α. For the highest plasma density shown ($\alpha = 0.01, \omega_{pe} = 10|\Omega_e|$), there is relatively little change in the value of E_k along each diffusion curve for resonant energies $E_k \gtrsim 100$ keV. Modest energy diffusion could occur at lower energy during scattering toward pitch angles ($\arctan(v_\perp/v_{||})$) near 90° because of cyclotron resonance with whistler mode waves for frequencies $\omega/|\Omega_e| \gtrsim 0.1$. As the thermal plasma density is decreased, the potential for substantial energy diffusion increases. For $\alpha = 0.1$, there is modest change in energy along each diffusion curve; this change is more pronounced for electron energies near 100 keV which resonate with whistler mode waves near a few tenths of the electron gyrofrequency. When $\alpha = 0.3$, the effects of significant energy diffusion extends to relativistic energies ($E_k \approx 1$ MeV). This allows whistler mode waves with frequencies $\omega/|\Omega_e| \geq 0.1$ to contribute to the stochastic acceleration of electrons in the high-energy tail of the plasma population.

As noted by *Gendrin* [1968], the diffusion curves in velocity space (left panels) demarcate the contours of

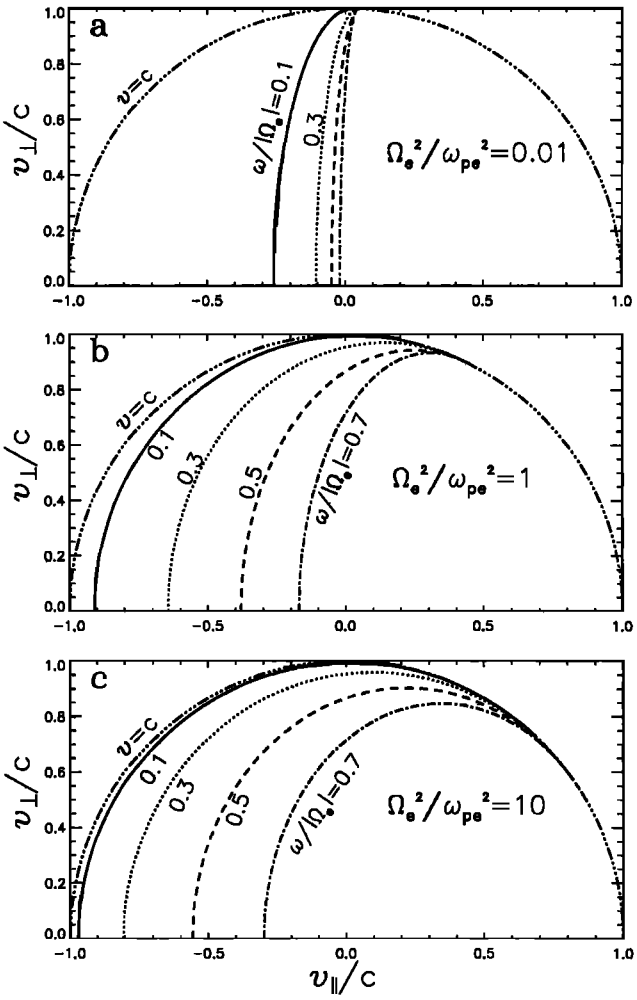

Figure 1. Resonant ellipses for first-order cyclotron resonant interaction between relativistic electrons and whistler mode waves as given by (9). Results are shown for five distinct wave frequencies and for three different locations characterized by the ratio $\omega_{pe}/|\Omega_e|$: (a) 0.01, (b) 1, and (c) 10.

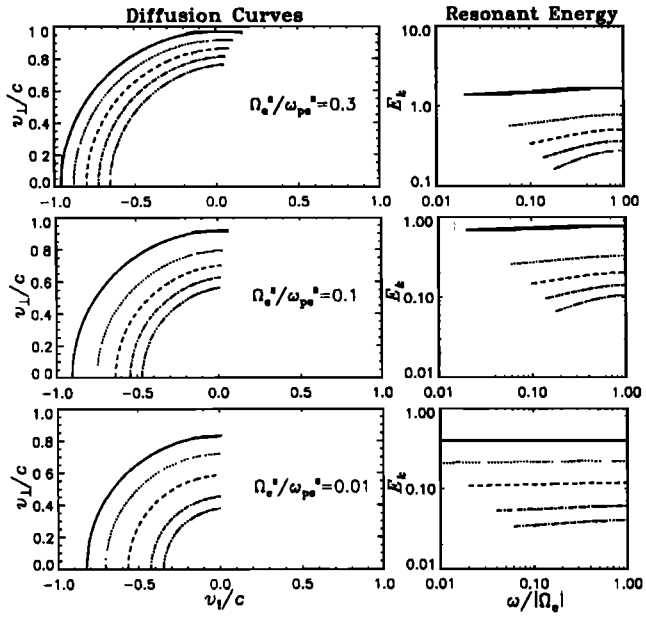

Figure 2. (left) Relativistic resonant diffusion curves for electron cyclotron resonant interaction with whistler mode waves in a moderately high density plasma. (right) Profiles of the resonant energy (in MeV) along each diffusion curve.

constant phase space density for marginal stability with respect to whistler mode waves. For any prescribed value of α, there is a natural tendency for the marginally stable distribution to become more anisotropic at lower energy. The injection of anisotropic medium energy electrons (10-100 keV) into the outer radiation zone during storm time conditions can lead to the excitation of intense whistler mode emissions [*Tsurutani and Smith*, 1977]. Because of propagation effects in the nonuniform magnetospheric plane, these waves can subsequently interact with higher-energy electrons under different magnetospheric conditions. If the high-energy population is initially isotropic, resonant diffusion will proceed toward 90° pitch-angle, thereby resulting in stochastic electron acceleration and concomitant wave attenuation. This mechanism provides a natural process for channeling energy from the storm time ring current population (10–100 keV), which originates from enhanced convective activity, into the high-energy tail of the electron distribution.

The region exterior to the plasmapause is characterized by low plasma density ($\alpha \geq 1$), particularly at night and at higher geomagnetic latitudes. When $\omega_{pe} < |\Omega_e|$, electromagnetic R mode waves occur in three distinct branches, each with different propagation characteristics [e.g., *Horne and Thorne*, 1998]. These branches are the guided whistler mode with $\omega < \omega_{pe}$, the unguided Z mode with $\omega_{pe} \leq \omega \leq |\Omega_e|$, and the free-space RX mode with $\omega > |\Omega_e|$. The RX mode, which is subject to cyclotron maser instability in the auroral cavity [e.g., *Wu and Lee*, 1979], has a phase speed $u_{ph} > c$ and consequently will not be considered here. For strictly parallel propagation, the dispersive properties of the R mode whistler and Z mode branches merge smoothly at the plasma frequency. The distinct nature of these two modes is only apparent for oblique propagation. Solutions for the resonant diffusion curves for these two modes are shown in Figure 3. As a result of the larger Alfvén speed, cyclotron resonant energies are much larger than for the case when $\alpha < 1$. Resonant velocity curves tend to be close to the light semicircle, and it is therefore more useful to show solutions for the diffusion curves in momentum space (left panels). For $\alpha = 1$ (Figure 3c) the results continue the trend shown in Figure 2. The lower densities lead to a larger change in energy along each diffusion curve, particularly over the range between 100 keV and 1 MeV. When $\alpha = 3$ (Figure 3b) the potential for stochastic acceleration extends well into the highly relativistic regime ($E_k > 1$ MeV). There is a smooth transition between the whistler mode and Z mode at $\omega/|\Omega_e| \approx 0.58$. The whistler mode ($\omega/|\Omega_e| \lesssim 0.58$) should be particularly effective in the stochastic acceleration of electrons over the energy range between 100 keV and a few MeV. The resonant diffusion curves exhibit a sharp cusp, which leads to a maximum energy along each diffusion curve (right panels); this severely limits the potential for further acceleration by the Z mode branch. It is also doubtful whether this branch

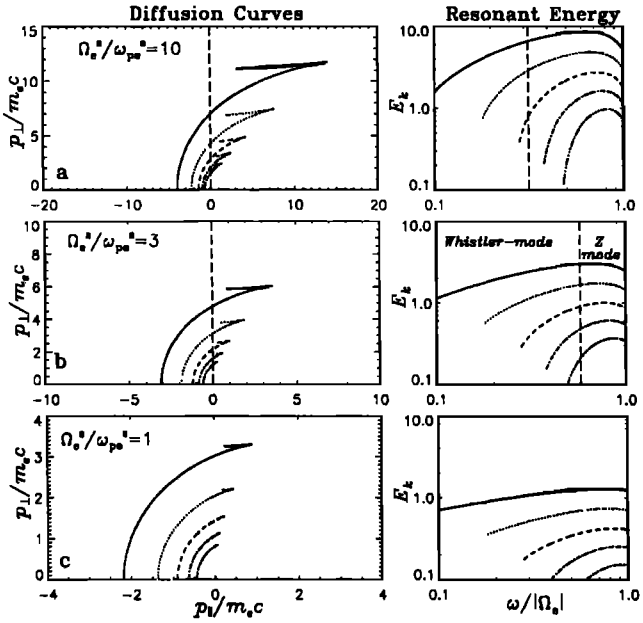

Figure 3. (left) Relativistic resonant diffusion curves in momentum space for electron cyclotron resonance with R mode waves in a low-density plasma. (right) Profiles of the resonant energy (in MeV) along each diffusion curve. In this case, the change in energy along each diffusion curve can be considerable.

could be excited in the outer magnetosphere during a storm. At even lower plasma density ($\alpha = 10$), resonance with the whistler mode branch is restricted to energies above 400 keV. The Z mode, which occurs for frequencies $\omega/|\Omega_e| > 0.33$, offers the possibility of electron acceleration over the important energy range between 100 keV and a few MeV. However, the source for the excitation of such waves needs to be identified.

7.2. *L* Mode Waves

The dispersive properties of electromagnetic ion cyclotron (EMIC) waves are strongly influenced by the composition of the plasma. In the present study, we adopt the ion composition given by $\eta_{H^+} = 0.77$, $\eta_{He^+} = 0.20$, $\eta_{O^+} = 0.03$ in the dispersion relation (19) [e.g., *Kozyra et al.*, 1984]. Equation (23) is then solved numerically to obtain the resonant electron diffusion curves. The results for the case of a high-density plasma, characteristic of the outer plasmasphere ($\alpha = 0.01$), are shown in Figure 4. In order to resonate with L mode waves, electrons must overtake the wave ($v_{||} > u$) with sufficient velocity to Doppler-shift the wave frequency ($\omega < \Omega_{H^+}$) up to $|\Omega_e|/\gamma$. The large Doppler-shift requires resonant velocities close to the speed of light. EMIC waves, as given by the dispersion relation (19) could, in principle, occur in three distinct frequency bands, but the waves observed in the Earth's high density plasmasphere preferentially occur in the band $\Omega_{O^+} \leq \omega \leq \Omega_{H_e^+}$ [*Anderson et al.*, 1992]. Resonant electron energies associated with such waves (Fig-

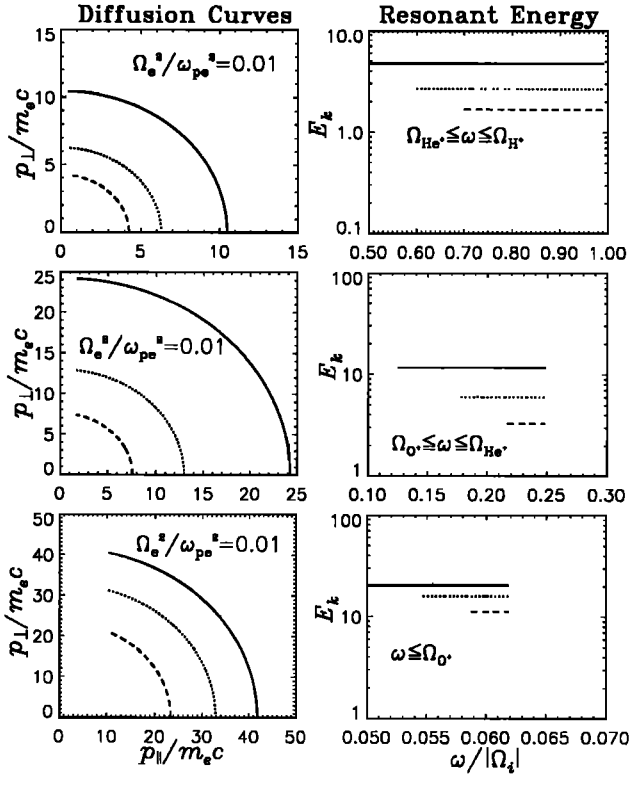

Figure 4. (left) Relativistic resonant diffusion curves for electron cyclotron resonant interaction with L mode EMIC waves in a high-density plasma. (right) Profiles of the resonant energy (in MeV) along each diffusion curve. Here changes in resonant energy are insignificant along each diffusion curve.

ure 4, right) are typically above 1 MeV, and there is very little energy change along the diffusion curves. Consequently, there will be little energy diffusion to accompany the rapid pitch angle scattering [*Thorne and Kennel*, 1971; *Lyons and Thorne*, 1972] associated with the large power spectral density of EMIC waves. The resonant diffusion curves in momentum space and the associated changes in electron energy for the case of a lower-density plasma (outside the plasmasphere) with $\alpha = 1.0$ are shown in Figure 5. Apart from an overall increase in the resonant energies for each EMIC wave branch, the results are similar to those in Figure 4. There is virtually no energy change along the diffusion curves. Such waves therefore appear to be ineffective as a mechanism for stochastic acceleration anywhere within the Earth's magnetosphere.

7.3. Nonrelativistic Case

Diffusion curves for nonrelativistic electrons interacting with R mode waves in an electron-proton plasma are shown in Figure 6. These curves are constructed from the analytical solutions (51) and (52), using the results of Appendix C and the cold plasma R mode dispersion relation (12). The results are shown for a relatively high-density plasma ($\alpha = 0.01$) to ensure that the scaling energy for resonant interaction, $E_M = B_0^2/(8\pi N_0) = \alpha E_0/2$, is well below the electron rest-mass energy $E_0 = m_e c^2$. For this choice of α, the nonrelativistic solutions obtained are essentially identical to the exact relativistic results presented above. Velocities along each diffusion curve (Figure 6a) have been normalized to the scaling velocity $v_M = (2E_M/m_e)^{1/2}$. The change in energy (normalized to $E_M \approx 2.5$ keV) along each curve is shown in Figure 6b. Significant energy change occurs only for $E \lesssim E_M$ during resonant interaction with relatively high-frequency whistler mode waves ($\omega/|\Omega_e| \gtrsim 0.4$). The absorption of such high frequency whistlers can cause significant energization, leading to an anisotropic distribution of suprathermal ($\lesssim 1$ keV) electrons (with peak flux near 90° pitch angle), as discussed by *Thorne and Horne* [1996].

The diffusion curves shown in Figure 6a also represent the marginally stable contours of electron phase space density [e.g., *Gendrin*, 1981]. These curves show slightly less anisotropy than the solutions presented by *Thorne and Horne* [1996] because of the erroneous assumption made in their analysis, as discussed in section 6. For larger values of $\alpha(\geq 0.1)$, the nonrelativistic approximation becomes invalid, and the solutions given by (51) and (52) are significantly different from the exact relativistic solutions discussed in section 7.1.

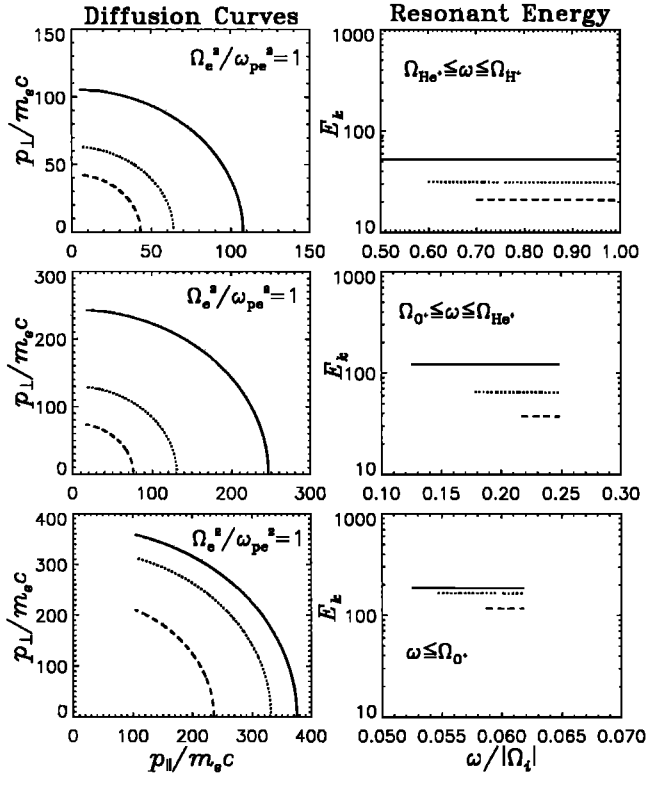

Figure 5. (left) Diffusion curves as in Figure 4, but for a lower-density plasma. (right) Profiles of the resonant energy along each diffusion curve. Resonant energies (in MeV) are higher than in Figure 4, and there is little energy change along each diffusion curve.

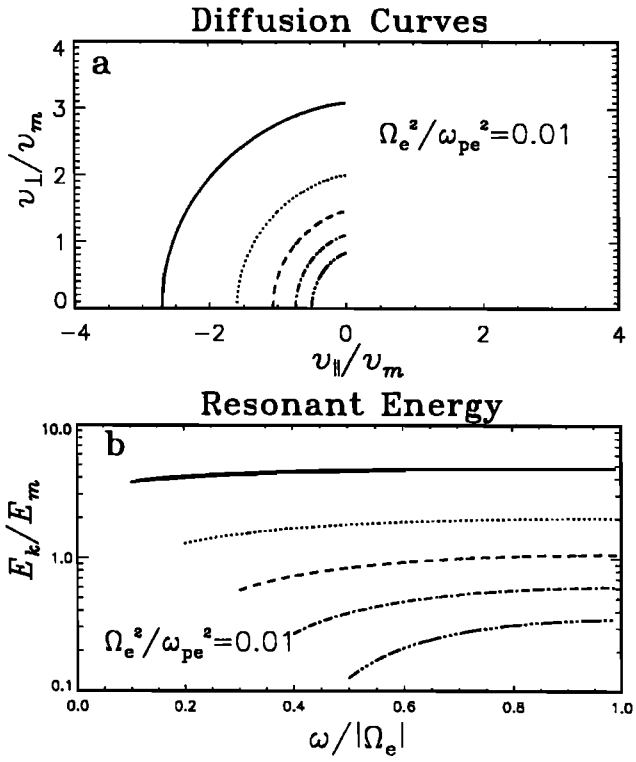

Figure 6. (a) Non-relativistic resonant diffusion curves for electrons interacting with R mode waves. (b) Profiles of resonant energy along each diffusion curve.

8. A Model for Stochastic Acceleration of Relativistic Electrons During Geomagnetic Storms

Enhanced convection electric fields provide the principal mechanism for the intensification of ring current (10–100 keV) flux during geomagnetic storms [*Lyons and Williams*, 1980; *Chen et al.*, 1994]. Inward convection also leads to an anisotropic distribution of the ring current ions and electrons which provides a source of free energy for the excitation of both EMIC waves [*Kozyra et al.*, 1997] and whistler mode waves respectively. The power spectral density of such waves is therefore enhanced considerably during a storm. Figure 7 provides a schematic description of the spatial region where enhanced levels of both EMIC waves and whistler mode chorus occur during a storm. EMIC waves are preferentially excited along the duskside plasmapause [*Jordanova et al*, 1997; *Kozyra et al.*, 1997] by the convective injection of ring current H^+. The zone of most intense wave activity is spatially localized because of the decrease in resonant energy [*Cornwall et al.*, 1970; *Perraut et al.*, 1976] and wave guiding by strong density gradients [*Thorne and Horne*, **1996]** associated with the plasmapause. Typical storm time EMIC wave amplitudes are in the range 1–10 nT [B. J. Anderson, private communication, 1998]. Whistler mode chorus emissions with frequencies $\omega/|\Omega_e| = 0.1 - 0.7$ can be excited by cyclotron resonance with anisotropic 10–100-keV electrons over a broad range of local times (2200–0900 magnetic local time (MLT)) in the region exterior to the storm time plasmapause [*Tsurutani and Smith*, 1974, 1977; *Koons and Roeder*, 1990; *Parrot and Gaye*, 1994]. Typical "chorus" wave amplitudes are in the range 10–100 pT, but occasionally the wave amplitude approaches $B_w = 1$ nT [*Parrot and Gaye*, 1994]. Relativistic electrons ($E_k \gtrsim 1$ MeV) have approximately circular drift paths which, for $L \approx 4$ to $L \approx 5$, traverse the zone of chorus emission from 2200 to 0900 MLT and also pass briefly through the duskside region of intense EMIC waves. The drift time for 1 MeV electrons near $L = 4.5$ is approximately 14 min. Such electrons have the potential to interact with whistler mode chorus for over 50% of their orbit, but only a few percent of the orbit lies within the zone of intense EMIC waves. The timescale for strong diffusion scattering loss, $\tau_{SD} \approx \tau_B/3\alpha_L^2$ (where τ_B is the bounce time and α_L is the loss cone size), is approximately 1 min for 1 MeV electrons at $L = 4.5$. Wave amplitudes required for strong diffusion scattering of 1 MeV electrons at this location are approximately $B_{SD} = 750$ pT [*Thorne*, 1983]. The average amplitudes of outer zone chorus emissions are usually well below this, resulting in weak diffusion scattering. In contrast, EMIC waves normally have amplitudes $B_w > B_{SD}$, but such waves are only present in a limited region near dusk. Consequently, the electron loss should occur gradually over many drift orbits.

On the basis of the diffusion curves presented in section 7 and observational information on wave activity (Figure 7), we propose the following model for the variation of relativistic electron flux during storms.

8.1. Main Phase Flux Depletion

During the main phase of a storm, intense EMIC waves are excited along the duskside plasmapause as a result of cyclotron resonance with anisotropic ring current H^+ ions [*Kozyra et al.*, 1997]. These waves can cause rapid pitch angle scattering of trapped ($\gtrsim 1$ MeV) electrons [*Thorne and Kennel*, 1971; *Lyons and Thorne*, 1972]; this scattering should contribute to the main phase depletion of relativistic electrons throughout the outer zone. Even though the intensity of storm time EMIC waves is above the level required for strong diffusion scattering, the limited spatial region of scattering should result in a loss time in excess of one hour. *Li et al.* [1997a] have shown that although the main phase depletion can partially be explained as an adiabatic response to ambient magnetic field change, additional loss is required to account for observed changes.

8.2. Recovery Phase Electron Acceleration

Substorm activity during the storm recovery can excite chorus emissions in the outer magnetosphere and also can maintain modest levels of EMIC waves inside

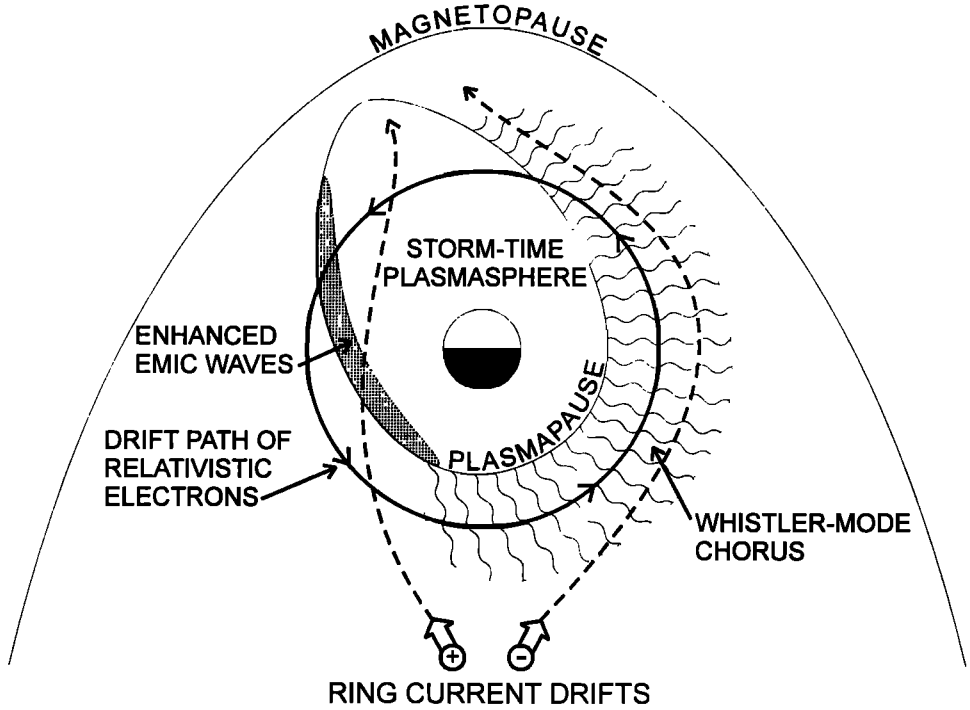

Figure 7. Schematic diagram showing spatial distribution of whistler mode chorus and EMIC waves during magnetic storms in relation to the position of the plasmapause and the drift paths of ring current (10–100 keV) electrons and ions and relativistic ($\gtrsim$ 1 MeV) electrons.

the plasmapause. Relativistic outer zone electrons can interact with both classes of waves leading to diffusion in pitch angle and energy. The diffusion curves presented in section 7 are given for a prescribed set of plasma parameters corresponding to particular spatial locations. However, electromagnetic waves in the magnetosphere readily propagate from their source of origin to other locations where plasma conditions can be quite different [e.g., *Horne and Thorne*, 1993, 1994; *Thorne and Horne*, 1996]. This allows the waves to interact resonantly with electrons over a broad energy range along the ray trajectory. A complete treatment of the consequences of resonant scattering requires a bounce-averaged analysis of diffusion over the motion of geomagnetically trapped electrons [e.g., *Lyons et al.*, 1972; *Abel and Thorne*, 1998]. Such a treatment is beyond the scope of the present study, which is directed toward the identification of the wave modes (and their location in the magnetosphere) that have the potential for producing substantial stochastic electron acceleration.

The most significant electron energy diffusion occurs during resonant interactions with whistler mode waves in regions of relatively low plasma density ($\alpha \gtrsim 1.0$) (Figure 3). Resonant electrons diffuse in velocity space until the contours of phase space density lie along the diffusion surfaces [*Gendrin*, 1968]. Wave-particle scattering produces a relativistic electron population with a "pancake" distribution (namely a distribution peaked at pitch angles near 90°) as the flux recovers following a storm; this anisotropic distribution is consistent with observations [e.g., *Ingraham et al.*, 1996]. Pitch angle scattering by EMIC waves tends to reduce the resonant electron anisotropy while conserving the electron energy (Figure 4). The scattering by EMIC waves near the duskside plasmapause (Figure 7) could be important since it would maintain an electron distribution which is more isotropic than that associated with resonant diffusion during electron-whistler interactions (Figures 2 and 3). Subsequent interaction with whistler mode chorus in the region outside the plasmapause would therefore cause further diffusion of relativistic electrons toward pitch angles near 90° and lead to additional electron acceleration. We suggest that a combination of energy diffusion by cyclotron-resonant absorption of whistlers together with pitch angle scattering by EMIC waves could provide a viable mechanism to account for the stochastic acceleration of electrons from energies near a few 100 keV to relativistic energies > 1 MeV over a period of a few days during the storm recovery. The rate of electron acceleration is primarily controlled by the average power spectral density of available whistler mode waves. Detailed bounce-averaged calculations of the rate of scattering are required in order to determine whether the suggested model could account for the observed electron acceleration during the recovery phase of a storm.

9. Conclusions

Diffusion curves for resonant electron interactions with field-aligned electromagnetic waves have been con-

structed for a range of plasma parameters representative of the storm time magnetosphere. Analytical solutions for the diffusion curves have been obtained for the idealized case of a single-ion cold plasma. A numerical method has been used for the more general case of a multi-ion plasma, and the numerical results are found to be identical to the analytical solution for the case of a single-ion plasma. This provides an important test of the accuracy of the numerical method, and gives reassurance that the method can be extended to treat situations where the wave dispersion relation is more complex (e.g., where the plasma is treated as hot, or where oblique wave propagation and other harmonic resonances need to be considered).

Our principal conclusions are as follows:

1. Significant electron energy diffusion can occur, leading to a "pancake" pitch angle distribution during resonant interactions with whistler mode waves. The potential for energization is most pronounced in regions of relatively low plasma density ($\alpha \gtrsim 1.0$).

2. EMIC (L mode) waves are also able to resonate with electrons in the energy range above 1 MeV, but the electron energies remain approximately constant along the resonant diffusion curves. Such waves could provide an important source of scattering loss for relativistic electrons during the main phase of a storm [*Thorne and Kennel*, 1971].

3. A combination of energy diffusion by whistler mode chorus and pitch angle scattering by EMIC waves could provide a viable mechanism to account for the gradual local stochastic acceleration of electrons from a few 100 keV to above 1 MeV in the outer magnetosphere ($L \approx 4$ to $L \approx 5$) during the recovery phase of a storm. Detailed calculations including bounce-averaged rates of diffusion are required to establish the timescale for this process.

Appendix A: Explicit Forms for f(ω) and g(ω) Appearing in Solution (34)

A1. *R* Mode (Dispersion Relation (12))

$$\begin{aligned} f(\omega) &= c_1\{A_1 \sin^{-1}(\frac{\omega - b_1}{a_1}) \\ &+ \frac{(B_1 - C_1)a_1 + (B_1 + C_1)(\omega - b_1)}{[a_1^2 - (\omega - b_1)^2]^{1/2}} \\ &+ \frac{[D_1(a_1^2 - b_1^2) - E_1 b_1]}{(a_1^2 - b_1^2)^{3/2}} \\ &\log_e \left| \frac{b_1(\omega - b_1) + [a_1 - (a_1^2 - b_1^2)^{1/2}]F_1}{b_1(\omega - b_1) + [a_1 + (a_1^2 - b_1^2)^{1/2}]F_1} \right| \\ &- E_1 \frac{[a_1^2 - (\omega - b_1)^2]^{1/2}}{(a_1^2 - b_1^2)\omega} \} \end{aligned} \quad \text{(A1)}$$

$$g(\omega) = \frac{[\alpha(1+\varepsilon)(1-\omega)(\omega+\varepsilon)]^{1/2}}{\omega[\alpha(1-\omega)(\omega+\varepsilon) + 1 + \varepsilon]} \quad \text{(A2)}$$

$$a_1 = [(1 + \alpha\varepsilon + \varepsilon)/\alpha + (1-\varepsilon)^2/4]^{1/2}$$
$$b_1 = (1-\varepsilon)/2$$
$$c_1 = (2a_1^2)^{-1}\alpha^{-1/2}(1+\varepsilon)^{-1/2}$$
$$A_1 = -2\alpha a_1^2$$

$$B_1 = \alpha(a_1 + b_1)^2 - 2\alpha(1-\varepsilon)(a_1 + b_1)$$
$$+\alpha(1 - 4\varepsilon + \varepsilon^2) + (1-\varepsilon)(1 + 4\alpha\varepsilon + \varepsilon)$$
$$(a_1 + b_1)^{-1}/2 + \varepsilon(1 + \alpha\varepsilon + \varepsilon)(a_1 + b_1)^{-2}$$

$$C_1 = \alpha(a_1 - b_1)^2 + 2\alpha(1-\varepsilon)(a_1 - b_1) + \alpha(1 - 4\varepsilon + \varepsilon^2)$$
$$-(1-\varepsilon)(1 + 4\alpha\varepsilon + \varepsilon)(a_1 - b_1)^{-1}/2$$
$$+\varepsilon(1 + \alpha\varepsilon + \varepsilon)(a_1 - b_1)^{-2}$$

$$D_1 = -b_1(A_1 + B_1 + C_1) - 2\alpha\varepsilon a_1^2 b_1^{-1} + 2\alpha b_1^3$$
$$-4\alpha(1-\varepsilon)b_1^2 + 2\alpha(1 - 4\varepsilon + \varepsilon^2)b_1$$
$$+(1-\varepsilon)(1 + 4\alpha\varepsilon + \varepsilon) + 2\varepsilon(1 + \alpha\varepsilon + \varepsilon)b_1^{-1}$$

$$E_1 = 2\alpha\varepsilon a_1^2$$

$$F_1 = \{a_1 + [a_1^2 - (w - b_1)^2]^{1/2}\}$$

A2. *L* Mode (Dispersion Relation (13))

$$\begin{aligned} f(\omega) &= c_2\{A_2 \sin^{-1}(\frac{\omega + b_2}{a_2}) \\ &+ \frac{(B_2 - C_2)a_2 + (B_2 + C_2)(\omega + b_2)}{[a_2^2 - (\omega + b_2)^2]^{1/2}} \\ &+ \frac{[D_2(a_2^2 - b_2^2) + E_2 b_2]}{(a_2^2 - b_2^2)^{3/2}} \\ &\log_e \left| \frac{b_2(\omega + b_2) - [a_2 - (a_2^2 - b_2^2)^{1/2}]F_2}{b_2(\omega + b_2) - [a_2 + (a_2^2 - b_2^2)^{1/2}]F_2} \right| \\ &- E_2 \frac{[a_2^2 - (\omega + b_2)^2]^{1/2}}{(a_2^2 - b_2^2)\omega} \} \end{aligned} \quad \text{(A3)}$$

$$g(\omega) = \frac{[\alpha\varepsilon(1+\varepsilon)(1+\varepsilon\omega)(1-\omega)]^{1/2}}{\omega[\alpha\varepsilon(1+\varepsilon\omega)(1-\omega) + 1 + \varepsilon]} \quad \text{(A4)}$$

$$a_2 = [(1 + \alpha\varepsilon + \varepsilon)/\alpha + (1-\varepsilon)^2/4]^{1/2}/\varepsilon$$
$$b_2 = (1-\varepsilon)/(2\varepsilon)$$
$$c_2 = (2a_2^2\varepsilon^2)^{-1}\alpha^{-1/2}(1+\varepsilon)^{-1/2}$$
$$A_2 = -2\alpha\varepsilon^3 a_2^2$$

$$B_2 = \alpha\varepsilon^3(a_2 - b_2)^2 + 2\alpha\varepsilon^2(1-\varepsilon)(a_2 - b_2)$$
$$+\alpha\varepsilon(1 - 4\varepsilon + \varepsilon^2) - (1-\varepsilon)(1 + 4\alpha\varepsilon + \varepsilon)(a_2 - b_2)^{-1}/2$$
$$(1 + \alpha\varepsilon + \varepsilon)(a_2 - b_2)^{-2}$$

$$C_2 = \alpha\varepsilon^3(a_2+b_2)^2 - 2\alpha\varepsilon^2(1-\varepsilon)(a_2+b_2)$$
$$+\alpha\varepsilon(1-4\varepsilon+\varepsilon^2) + (1-\varepsilon)(1+4\alpha\varepsilon+\varepsilon)(a_2+b_2)^{-1}/2$$
$$+(1+\alpha\varepsilon+\varepsilon)(a_2+b_2)^{-2}$$

$$D_2 = b_2(A_2+B_2+C_2) + 2\alpha\varepsilon^2 a_2^2 b_2^{-1} - 2\alpha\varepsilon^3 b_2^3$$
$$+4\alpha\varepsilon^2(1-\varepsilon)b_2^2 - 2\alpha\varepsilon(1-4\varepsilon+\varepsilon^2)b_2$$
$$-(1-\varepsilon)(1+4\alpha\varepsilon+\varepsilon) - 2(1+\alpha\varepsilon+\varepsilon)b_2^{-1}$$

$$E_2 = 2\alpha\varepsilon^2 a_2^2$$

$$F_2 = \{a_2 + [a_2^2 - (\omega+b_2)^2]^{1/2}\}$$

Appendix B: Explicit Form of (23) for the Multi-ion Dispersion Relation (19)

We solve

$$\frac{dv_{||}}{d\omega} = -\left(\frac{1-uv_{||}}{1-u^2}\right)\left[v_{||}Q + \frac{(v_{||}-u)}{\omega}\right] \quad \text{(B1)}$$

where

$$Q = \frac{P_0+P_1+P_2+P_3}{2\omega^2[\alpha\varepsilon P + p_1\omega^2 + p_2\omega + p_3]}$$

$$P_0 = (1+2\varepsilon\omega)(1-\omega)(4\omega-1)(16\omega-1)(1+\varepsilon\omega)^{-1}$$
$$P_1 = \eta_1(2\omega-1)(1+\varepsilon\omega)(4\omega-1)(16\omega-1)(1-\omega)^{-1}$$
$$P_2 = \eta_2(8\omega-1)(1+\varepsilon\omega)(1-\omega)(16\omega-1)(4\omega-1)^{-1}$$
$$P_3 = \eta_3(32\omega-1)(1+\varepsilon\omega)(1-\omega)(4\omega-1)(16\omega-1)^{-1}$$

and u, P, p_1, p_2, p_3 are given by (19)–(21).

Appendix C: Explicit Forms for the Functions F and G Appearing in Solution (51)-(52)

C1. *R* Mode (Dispersion Relation (12))

$$F(\omega) = \left(\frac{1+\varepsilon}{\alpha}\right)[R_1\log_e\omega - S_1\log_e(a_1+b_1-\omega) + \frac{T_1}{(a_1+b_1-\omega)} + U_1\log_e(a_1-b_1+\omega) - \frac{V_1}{a_1-b_1+\omega}] - \frac{u^2}{\omega^2} \quad \text{(C1)}$$

$$R_1 = (1-\varepsilon)/(a_1^2-b_1^2)^2$$
$$S_1 = [(1-\varepsilon)(2a_1+b_1) - 2(a_1+b_1)^2]/[4a_1^3(a_1+b_1)^2]$$
$$T_1 = [1-\varepsilon-2(a_1+b_1)]/[4a_1^2(a_1+b_1)]$$
$$U_1 = -[(1-\varepsilon)(2a_1-b_1) + 2(a_1-b_1)^2]/[4a_1^3(a_1-b_1)^2]$$
$$V_1 = -[1-\varepsilon+2(a_1-b_1)]/[4a_1^2(a_1-b_1)]$$

$$G(\omega) = -u(1-\omega)/\omega \quad \text{(C2)}$$

C2. *L* Mode (Dispersion Relation (13))

$$F(\omega) = \left(\frac{1+\varepsilon}{\alpha\varepsilon^4}\right)[R_2\log_e\omega - S_2\log_e(a_2-b_2-\omega) + \frac{T_2}{(a_2-b_2-w)} + U_2\log_e(a_2+b_2+\omega) - \frac{V_2}{(a_2+b_2+\omega)}] - \frac{u^2}{\varepsilon^2\omega^2} \quad \text{(C3)}$$

$$R_2 = (1-\varepsilon)/(a_2^2-b_2^2)^2 a$$
$$S_2 = [(1-\varepsilon)(2a_2-b_2) + 2\varepsilon(a_2-b_2)^2]/[4a_2^3(a_2-b_2)^2]$$
$$T_2 = [1-\varepsilon+2\varepsilon(a_2-b_2)]/[4a_2^2(a_2-b_2)]$$
$$U_2 = [2\varepsilon(a_2+b_2)^2 - (1-\varepsilon)(2a_2+b_2)]/[4a_2^3(a_2+b_2)^2]$$
$$V_2 = [-(1-\varepsilon) + 2\varepsilon(a_2+b_2)]/[4a_2^2(a_2+b_2)]$$

$$G(\omega) = u(1+\varepsilon\omega)/(\varepsilon\omega) \quad \text{(C4)}$$

The parameters a_1, b_1 appearing in (C1) and the parameters a_2, b_2 in (C3) are as defined in Appendix A. The solutions given in Appendix C are similar to those given by *Gendrin and Roux* [1980] and *Gendrin* [1981].

Acknowledgments. D.S. acknowledges support from the Natural Sciences and Engineering Research Council of Canada under grant A-0621. The work was also supported by NSF grant ATM 97-29021, NASA grant NAG5 4680, and NATO grant CRG 970575.

The Editor thanks A. Johnstone and X. Li for their assistance in evaluating this paper.

References

Abel, B., and R. M. Thorne, Electron scattering loss in Earth's inner magnetosphere, 1, Dominant physical processes, *J. Geophys. Res.*, *103*, 2385, 1998.

Anderson, B. J., R. E. Erlandson, and L. J. Zanetti, A statistical study of Pc 1-2 magnetic pulsations in the equatorial magnetosphere, 2, Wave properties, *J. Geophys. Res.*, *97*, 3089, 1992.

Baker, D. N., J. B. Blake, R. W. Klebesadel, and P. R. Higbie, Highly relativistic electrons in the Earth's outer magnetosphere, 1, Lifetimes and temporal history 1979-1984, *J. Geophys. Res.*, *91*, 4265, 1986.

Baker, D. N., J. B. Blake, L. B. Callis, J. R. Cummings, D. Hovestadt, S. Kanekal, B. Blecker, R. A. Mewaldt, and R. D. Zwickl, Relativistic electron acceleration and

decay time scales in the inner and outer radiation belts: SAMPEX, *Geophys. Res. Lett.*, *21*, 409, 1994.

Blake, J. B., D. N. Baker, N. Turner, K. W. Ogilvie, and R. P. Lepping, Correlation of changes in the outer zone relativistic-electron population with upstream solar wind and magnetic field measurements, *Geophys. Res. Lett.*, *24*, 927, 1997.

Chen, M. W., L. R. Lyons, and M. Schulz, Simulation of phase space distribution of storm time proton ring current, *J. Geophys. Res.*, *99*, 5745, 1994.

Cornwall, J. M., F. V. Coroniti, and R. M. Thorne, Turbulent loss of ring current protons, *J. Geophys. Res.*, *75*, 4699, 1970.

Gendrin, R., pitch angle diffusion of low-energy protons due to gyro-resonant interaction with hydromagnetic waves, *J. Atmos. Terr. Phys.*, *30*, 1313, 1968.

Gendrin, R., General relationships between wave amplification and particle diffusion in a magnetoplasma, *Rev. Geophys.*, *19*, 171, 1981.

Gendrin, R., and A. Roux, Energization of helium ions by proton-induced hydromagnetic waves, *J. Geophys. Res.*, *85*, 4577, 1980.

Horne, R. B., and R. M. Thorne, On the preferred source location for the convective amplification of ion-cyclotron waves, *J. Geophys. Res.*, *98*, 9223, 1993.

Horne, R. B., and R. M. Thorne, Convective instabilities of electromagnetic ion cyclotron waves in the outer magnetosphere, *J. Geophys. Res.*, *99*, 17259,1994.

Horne, R. B., and R. M. Thorne, Potential waves for relativistic electron scattering and stochastic acceleration during magnetic storms, ***Geophys. Res. Lett., 25,* 3011,** 1998.

Ince, E. L., *Ordinary Differential Equations*, p. 23, **Dover,** NY, 1944.

Ingraham, J. C., T. E. Cayton, R. D. Belian, R. A. Christiansen, F. Guyker, M. M. Meier, G. D. Reeves, D. H. Brautigan, M. S. Gussenhoven, and R. M. Robinson, Multisatellite characterization of the large energetic electron flux increase at L=4-7, in the five-day period following the March 24, 1991, solar energetic particle event, in *Workshop on the Earth's Trapped Particle Environment*, edited by G. D. Reeves, p. 103, AIP Press, Woodbury, New York, 1996.

Jordanova, V. K., J. U. Kozyra, A. F. Nagy, and G. V. Khazanov, Kinetic model of the ring current-atmosphere interactions, *J. Geophys. Res.*, *102*, 14279, 1997.

Kennel, C. F., and F. Engelmann, Velocity space diffusion from weak plasma turbulence in a magnetic field, *Phys. Fluids*, *9*, 2377, 1966.

Koons, H. C., and J. L. Roeder, A survey of equatorial magnetospheric wave activity between 5 and 8 R_E, *Planet. Space Sci.*, *38*, 1335, 1990.

Kozyra, J. U., T. E. Cravens, A. F. Nagy, E. G. Fontheim, and R. S. B. Ong, Effects of energetic heavy ions on electromagnetic ion cyclotron wave generation in the plasmapause region, *J. Geophys. Res.*, *89*, 2217, 1984.

Kozyra, J. U., V. K. Jordanova, R. B. Horne, and R. M. Thorne, Modeling of the contribution of electromagnetic ion cyclotron (EMIC) waves to stormtime ring current erosion, in *Magnetic Storms*, *Geophys. Monogr. Ser.*, Vol. 98, edited by B. T. Tsurutani et al., p. 187, AGU, Washington, D.C., 1997.

Li, X., I. Roth, M. Temerin, J. R. Wygant, M. K. Hudson, and J. B. Blake, Simulation of the prompt energization and transport of radiation belt particles during the March 24, 1991 SSC, *Geophys. Res. Lett.*, *20*, 2423, 1993.

Li, X., D. N. Baker, M. Temerin, T. E. Cayton, E. G. D. Reeves, R. A. Christensen, J. B. Blake, M. D. Looper, R. Nakamura, and S. G. Kanekal, Multisatellite observations of the outer zone electron variation during the November 3–4, 1993, magnetic storm, *J. Geophys. Res.*, *102*, 14123, 1997a.

Li, X., D. N. Baker, M. Temerin, D. Larson, R. P. Lin, G. D. Reeves, M. Looper, S. G. Kanekal, and R. A. Mewaldt, Are energetic electrons in the solar wind the source of the outer radiation belt?, *Geophys. Res. Lett.*, *24*, 923, 1997b.

Lyons, L. R., and R. M. Thorne, Parasitic pitch angle diffusion of radiation belt particles by ion cyclotron waves, *J. Geophys. Res.*, *77*, 5608, 1972.

Lyons, L. R., and D. J. Williams, A source for the geomagnetic storm main phase ring current, *J. Geophys. Res.*, *85*, 523, 1980.

Lyons, L. R., R. M. Thorne, and C. F. Kennel, pitch angle diffusion of radiation belt electrons within the plasmasphere, *J. Geophys. Res.*, *77*, 3455, 1972.

Nishida, A., Outward diffusion of energetic particles form the Jovian radiation belt, *J. Geophys. Res.*, *81*, 1771, 1976.

Parrot, M., and C. A. Gaye, A statistical survey of ELF waves in a geostationary orbit, *Geophys. Res. Lett.*, *21*, 2463, 1994.

Paulikas, G. A., and J. B. Blake, Effects of the solar wind on magnetospheric dynamics: Energetic electrons at the synchronous orbit, in *Quantitative Modeling of Magnetospheric Processes*, *Geophys. Monogr. Ser.*, Vol. 21, edited by W. P. Olsen, p. 180, AGU, Washington, D. C., 1979.

Perraut, S., R. Gendrin, and A. Roux, Amplification of ion-cyclotron waves for various typical radial profiles of magnetospheric parameters, *J. Atmos. Terr. Phys.*, *38*, 1191, 1976.

Schulz, M., and L. Lanzerotti, *Particle Diffusion in the Radiation Belts*, Springer-Verlag, New York, 1974.

Stix, T. H., *The Theory of Plasma Waves*, McGraw-Hill, New York, 1962.

Swanson, D. G., *Plasma Waves*, Academic, San Diego, Calif., 1989.

Temerin, M., I. Roth, M. K. Hudson, and J. R. Wygant, New paradigm for the transport and energization of radiation belt particles, *Eos, Trans., AGU*, Fall Meet. Suppl., *75* (44), 538, 1994.

Thorne, R. M., Microscopic plasma processes in the Jovian magnetosphere, in *Physics of the Jovian Magnetosphere*, edited by A. J. Dessler, p. 454, Cambridge Univ. Press, New York, 1983.

Thorne, R. M., and R. B. Horne, Whistler absorption and electron heating near the plasmapause, *J. Geophys. Res.*, *101*, 4917, 1996.

Thorne, R. M., and C. F. Kennel, Relativistic electron precipitation during magnetic storm main phase, *J. Geophys. Res.*, *76*, 4446, 1971.

Tsurutani, B. T., and E. J. Smith, Postmidnight chorus: A substorm phenomenon, *J. Geophys. Res.*, *79*, 118, 1974.

Tsurutani, B. T., and E. J. Smith, Two types of magnetospheric ELF chorus and their substorm dependences, *J. Geophys. Res.*, *82*, 5112, 1977.

Walker, A. D. M., *Plasma Waves in the Magnetosphere*, Springer-Verlag, New York, 1993.

Wu, C. S., and L. C. Lee, A theory of the terrestrial kilometric radiation, *Astrophys. J.*, *230*, 621, 1979.

D. Summers, Department of Mathematics and Statistics, Memorial University of Newfoundland, St. John's, Newfoundland, Canada A1C 5S7. (e-mail: dsummers@math.mun.ca)

R. M. Thorne, Department of Atmospheric Sciences, University of California, P. O. Box 951565, Los Angeles, CA 90095-1565. (e-mail: rmt@atmos.ucla.edu)

F. Xiao, Department of Physics and Astronomy, University of California, P. O. Box 951547, Los Angeles, CA 90095-1547. (e-mail: xiao@physics.ucla.edu)

(Received February 3, 1998; revised May 1, 1998; accepted May 15, 1998.)